JACS
JOURNAL OF THE AMERICAN CHEMICAL SOCIETY
Communication
Cite This: J. Am. Chem. Soc. 2019, 141, 12182−12186
pubs.acs.org/JACS

Inversion of Dispersion: Colloidal Stability of Calixarene-Modified Metal−Organic Framework Nanoparticles in Nonpolar Media

Uiseok Jeong,[†] Nesibe A. Dogan,[‡] Mousumi Garai,[†] Thien S. Nguyen,[†] J. Fraser Stoddart,[§,∥,⊥] and Cafer T. Yavuz*[,†,‡,#]

[†]Graduate School of EEWS and [‡]Department of Chemical and Biomolecular Engineering, Korea Advanced Institute of Science and Technology (KAIST), Daejeon 34141, Republic of Korea

[§]Department of Chemistry, Northwestern University, Evanston, Illinois 60208, United States

[∥]Institute for Molecular Design and Synthesis, Tianjin University, Tianjin 300072, P. R. China

[⊥]School of Chemistry, University of New South Wales, Sydney, NSW 2052 Australia

[#]Department of Chemistry, Korea Advanced Institute of Science and Technology (KAIST), Daejeon 34141, Republic of Korea

Supporting Information

ABSTRACT: Making metal−organic frameworks (MOFs) that are stabilized in nonpolar media is not as straightforward as making their inorganic nanoparticle counterparts, since surfactants penetrate through the porous structures or dissolve the secondary building units (SBUs) through ligand-exchange linker modulator mechanisms. Herein, we report that calixarenes stabilize UIO-66 nanoparticles effectively by remaining outside the grains through size exclusion, without pores becoming blocked, all the while providing amphiphilicity that permits the formation of stable colloidal dispersions with much narrower size distributions. Using the UIO-66 dispersed solutions, we show that smooth films from an otherwise immiscible polystyrene can be made feasibly.

Stable colloidal dispersions of nanoparticles are prerequisite to applications where active nanomaterials are expected to be uniformly distributed.[1] Metal−organic frameworks (MOFs) are now well-known to feature highly desired properties[2,3] such as very high surface areas,[4−6] accessible and tunable pores,[7,8] morphology control,[9−11] high thermal stability,[12−14] chemical stability for catalysis[15−18] and drug delivery applications.[19,20] MOFs are almost exclusively hydrophilic because they are made from positively charged nodes of secondary building units (SBUs) combined with negatively charged organic linkers.[21] This molecular arrangement leads to the necessity for using modulators to control their aqueous colloidal dispersions.[22,23] Dispersing MOFs in nonpolar media without altering linker coverage, however, is still an outstanding challenge.

A few groups have attempted the functionalization of MOF surfaces using hydrophobic ligands or by mixing with hydrophobic compounds, such as polydimethylsiloxane. Another approach entails carbonization through pyrolysis to provide shells for encapsulation.[24−26] These suspended MOFs suffer, however, from decreased adsorption capacity, loss of colloidal properties, lower catalytic activity, and adverse effects on their structures such as blocking of pore channels.[27,28] To solve these problems, we sought to find the right chemical agent that protects the porosity and accessibility of MOFs while giving them colloidal stability in nonpolar solvents. To the best of our knowledge, there is no generalized postsynthetic colloidal stabilization procedure to disperse MOFs in nonpolar media.

Macrocycle-based MOFs have been investigated by several groups. It is desirable to bring the macrocyclic and MOF components together because of the new properties that may result. Frameworks based on crown ethers, cyclodextrins,[29,30] calixarenes,[31] cucurbiturils, pillararenes, and other macrocycles are commonly encountered.[32−34] These materials have found various applications in heterogeneous catalysis, gas capture and storage, templated synthesis of inorganic porous materials, and molecular recognition, such as the selective capture of even NO_2.[35]

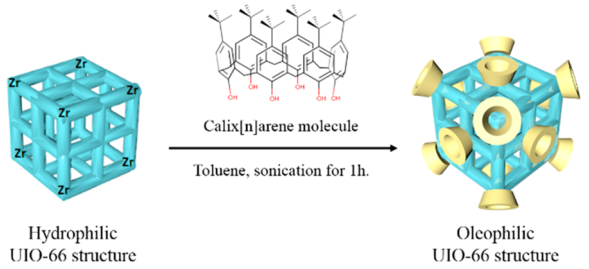

Figure 1. Inverting the polarity of UIO-66 by calixarene coating.

Calix[*n*]arenes (Cx)—well-known macrocycles with intrinsic pores—are easily and sustainably synthesized from formaldehyde and para-substituted phenols. Calix[*n*]arenes have basket-shaped conformations and different ring sizes, which depend on the synthetic conditions. In a typical calixarene, the lower rim is hydrophilic in nature mainly because of the phenolic functionalities. The upper rim is usually a dedicated hydrophobic cavity populated by aromatic functions and aliphatic side groups. If calixarenes could be stationed on the open metal sites of the external surfaces of

Received: April 18, 2019
Published: June 11, 2019

DOI: 10.1021/jacs.9b04198
J. Am. Chem. Soc. 2019, 141, 12182−12186

MOFs through the interaction with phenolic groups, the hydrophobic upper rims could provide desired oleophilicity, rendering a stable colloidal dispersion. The calixarene cavity would then permit facile transport of guests.

Here, we show a mild surface modification route, potentially applicable for any MOF, to disperse the coated MOF in nonpolar media while at the same time effectively refining the particle-size distribution below a stability maximum. We focused on UIO-66 with 4-*tert*-butylcalix[*n*]arenes since the size of the calixarene surfactants were comfortably larger than the pore openings (Figure 1). As-synthesized UIO-66 particles coated with different amounts of calix[*n*]arene (0 to 30 wt %) were investigated in nonpolar solvents, in this case, toluene. The resulting particles were characterized using gas adsorption isotherms, particle dispersities, and particle size distributions.

UIO-66 was synthesized according to a literature procedure[36] in which 5 mmol of terephthalic acid, 4 mmol of zirconium chloride (5:4 ratio), and 3 mL of HCl (35.5%) were mixed in 80 mL of dry DMF within a glass vial before being sealed with Teflon tape and heated at 120 °C for 24 h. We decided to evaluate UIO-66 as a suitable MOF system because it is known to be very stable (eliminating unwanted degradation during optimizations) and features pores of 0.8 and 1.1 nm, safely smaller than those of the tested calixarene molecule.[37] In a typical dispersion experiment, toluene solutions of 0−30% (w/w) calix[*n*]arene (where n = 4, 6 or 8) were mixed with different amounts of as-synthesized UIO-66 powders. After sonication, the particles were washed with toluene and centrifuged prior to characterization. Finally, the filtered calix[*n*]arene-coated UIO-66 particles were rinsed with toluene and dried under vacuum in the oven.

Among the calixarenes we tested, calix[6]arene came out as the expected optimal coating agent since its structure has larger pores than calix[4]arene while preserving its hollow conical shape without bending. Calix[8]arene is known to form more flexible structures than calix[4]arene and calix[6]arene, and metal complexes (transition and lanthanide) formed with calix[8]arene showed three special conformations: pleated loop,[38] double-cone,[39] and shell type, which wraps around a small cluster.[40] It is also evident from our initial testing that the use of calix[6]arene gave more suspended particles of UIO-66. Other MOFs, namely, HKUST-1 (Basolite C300) and MIL-53(Basolite A100), gave no detectable suspensions with calix[6]arene because of their larger-than-the-surfactant pore openings (Figure S1). The calix[6]arene-coated UIO-66 was found to be stable over 3 days whereas uncoated UIO-66 settled in just 5 min (Figures S2−S3, Supporting Movie).

When UIO-66 was suspended in calix[6]arene, it showed the characteristic Tyndall effect with a passing green laser beam (Figure 2). Upon variation of the calix[6]arene amount (0 to 30 wt %), we found that particle size distribution was the most uniform at 7.5 wt % with an average size of 132.2 ± 45.1 nm. Dynamic light scattering (DLS) profiles revealed that from 2.5 up to 15 wt %, calix[6]arene can suspend nanoparticles of UIO-66 (Figure S4). The particle size distribution follows a nonlinear trend that is best explained by the concentration dependence of the colloidal stability. The observed activity started after the addition of calixarenes (>1%), where large aggregated particle groups were coated with limited amounts of calixarenes, leading to a large particle-size distribution. The continued addition of calix[6]arene resulted in a maximum for the stabilized group (2.5%) but was still not enough to separate them to the smaller, more stable particle dispersion. The use of

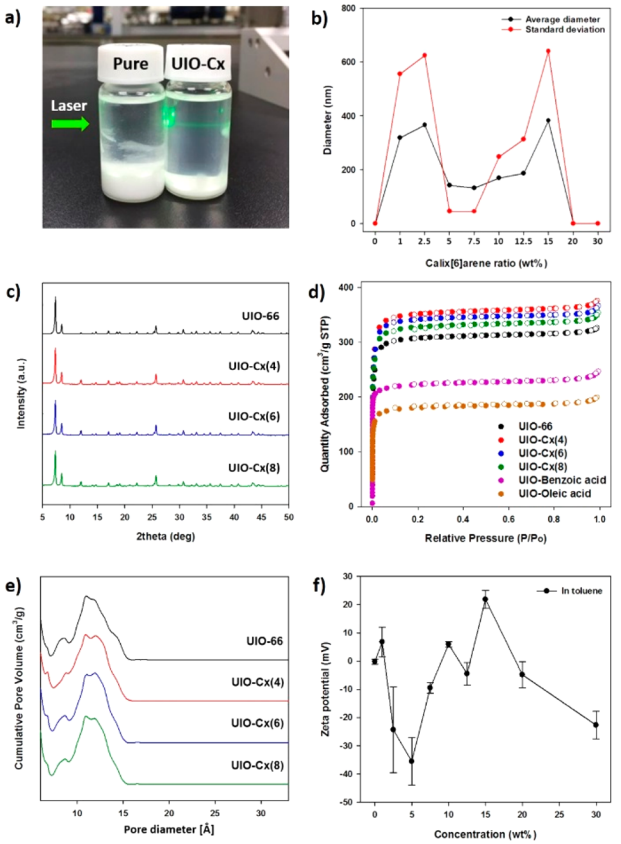

Figure 2. Characterization of calix[6]arene (Cx)-coated UIO-66 particles. (a) Typical *Tyndall* effect revealing colloidal dispersions (*pure* describes UIO-66 mixed with solvent only, while *UIO-Cx* denotes UIO-66 solution with 5% calix[6]arene), (b) particle size distributions measured with DLS after filtration through a 0.5-μm syringe filter, (c) XRD data of UIO-66 particles before and after coating with Cx, (d) BET specific surface areas using a N_2 probe at 77 K, (e) respective pore size distributions, and (f) zeta potential analysis of UIO-66 in the presence of increasing concentrations of the calixarene in toluene.

5∼7.5% calixarene provides sufficient coverage to stabilize many particles and also partially fragment the larger aggregates. In the plateau region (10−12.5%), there is a compromise between trying to stabilize more particulates vs multilayer-coated calixarenes for the already-stabilized particles. At 15%, there is enough calixarene to cover all the stabilized particles and to force a good amount of them to settle. Once the calixarene concentration reaches 20%, all stabilization is lost to a pure calixarene solution. As expected, the crystallinity of UIO-66 was not hindered or altered with calix[6]arene treatment (Figure 2c).

In order to verify the porosity of suspended UIO-66, we checked BET N_2 surface areas at 77 K. Interestingly, the nanoparticulate UIO-66 with calix[6]arene coating showed a higher surface area (1385 m^2/g) than native UIO-66 (1245 m^2/g) (Figure 2d). Since most modifications end up decreasing surface areas by either filling up the pores or blocking the openings, the preserved (or in this case even increased) surface area reveals the unperturbed nature of the framework. We verified this behavior further by using benzoic acid and oleic acid as common surfactants to produce colloidal dispersions of UIO-66 (Figure 2d). BET surface areas decreased 27.8% and 42.1% for benzoic acid and oleic acid,

DOI: 10.1021/jacs.9b04198
J. Am. Chem. Soc. 2019, 141, 12182−12186

respectively. Pore size distributions were also found to be preserved in each case for calixarene-coated particles (Figure 2e), adding further proof of untouched interiors. The FT-IR spectra remained identical, with 1398, 1577, 3469 cm^{-1} (Figure S5), 1398, and 1577 cm^{-1} peaks from COO^- groups and 3469 cm^{-1} from OH groups. It is important to note that the contribution of the −OH band resulting from calixarene coverage displayed a lower intensity than the structural carboxylates and also overlapped with them. Zeta potential measurements (Figure 2f) indicated considerable increase in particle dispersity upon addition of calixarenes, confirming the DLS measurements. In addition, dispersion stability analysis (Turbiscan) of the solutions provided no transmittance of the 880 nm light for the calix[6]arene-containing samples, indicating a highly saturated supernatant (Figure S6). Although all the characterizations point to the coating of the MOF grains with calixarenes, we wanted to obtain further proof for the presence of calix[6]arene coating on the UIO-66. For that, we first dissolved the composites in sulfuric acid (Figure S7) and recorded ^{1}H NMR spectra in DMSO-d_6 (Figure S8). Peaks observed at 7.1 and 7.4 ppm correlate only to the pure calix[6]arene. Another proof came from XPS characterization of the composites. Upon the increased addition of calix[6]arene, carbon content increased accordingly (Figure S9 and Table S1) while the presence of Zr and oxygen decreased.

Electron microscopy images of pure and calix[6]arene-treated solutions revealed suspended particles up to 15 wt % (Figure 3). When calix[6]arene exceeded 20 wt %, film-like deposits of calix[6]arene became dominant, also explaining why the optimal concentration is around 7.5 wt %. TEM images before and after coating also show a significant reduction in agglomeration (Figure S10). This result was also verified by Cryo-EM where a toluene solution that was frozen in liquid ethane showed individual particles widespread over a grid (Figure S11).

The colloidal suspension of UIO-66 with calix[6]arene is highly stable and, therefore, it could be cast as a mixed film using a polymer such as polystyrene, a scenario not previously possible with uncoated UIO-66.

When we mixed the stable suspension with toluene solutions of polystyrene, we achieved continuous films with high uniformity (Figure 4). In the absence of calixarene, however, the films formed cracks immediately and were extremely brittle. The distribution of MOF particles was also nonuniform. The EDX was used to identify elemental compositions of selected regions on the films (Figure S12). In this technique, particles observed by light contrast were confirmed to be UIO-66 and the darker areas were polystyrene. To further evaluate the polymer-MOF composites, we measured the tensile strength of the films and found that coating of UIO-66 increased the strain resistance of the polystyrene film by a factor of two (Figures S13−S15).

Gas (CO_2, CH_4, N_2) uptake properties of Cx-coated UIO-66 at 273 and 298 K were found to be in line with the BET surface areas (Figure S16). TGA analysis of calix[n]arene-coated UIO-66 also showed no noticeable changes when compared with the parent structure (Figure S17). In the case of oleic acid, however, a significant deviation in the thermal profile was observed. The lower stability of the structures followed the same pattern as UIO-66, demonstrating that the calix[n]arene does not hinder gas adsorption on UIO-66. Interestingly, benzoic acid-coated particles followed a similar stability curve as did the calixarene derivatives. Because oleic acid decomposes at a lower temperature, it is not a suitable surfactant. Retained weight percentage is lower in the case of linear surfactants since the carbon content is higher compared to calixarene versions.

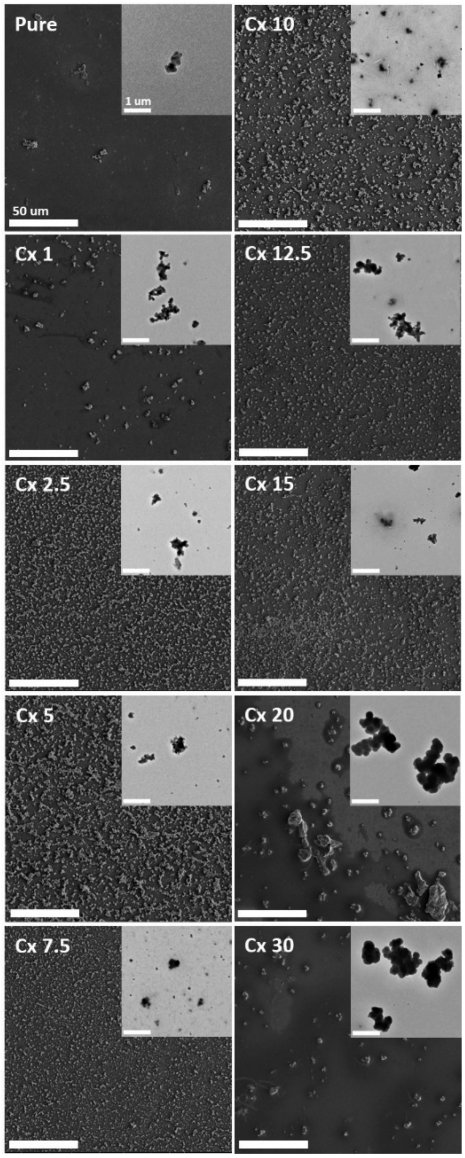

Figure 3. Electron microscopy images of calix[6]arene-coated UIO-66 particles. Scanning electron microscopy (SEM) images show uniform distribution through a wide area (scale bars are 50 μm). Transmission electron microscopy (TEM, insets) reveals individual particles that are consistent with the DLS measurements (scale bars are 1 μm, Pure means UIO-66 only, and Cx represents calix[6]arene-coated UIO-66 particles with wt % as shown with the arabic numerals).

In conclusion, we have shown that supramolecular amphiphilic macrocyclic structures can form stable colloidal dispersions of MOFs, provided that their hydrodynamic sizes are larger than the pore openings. The strategies employed here follow well-established practices[41] with precise tuning for the emerging materials. Our findings could lead to a universal methodology to form stable nonpolar dispersions of MOFs, particularly for use in mixed-matrix membranes.[42]

DOI: 10.1021/jacs.9b04198
J. Am. Chem. Soc. 2019, 141, 12182−12186

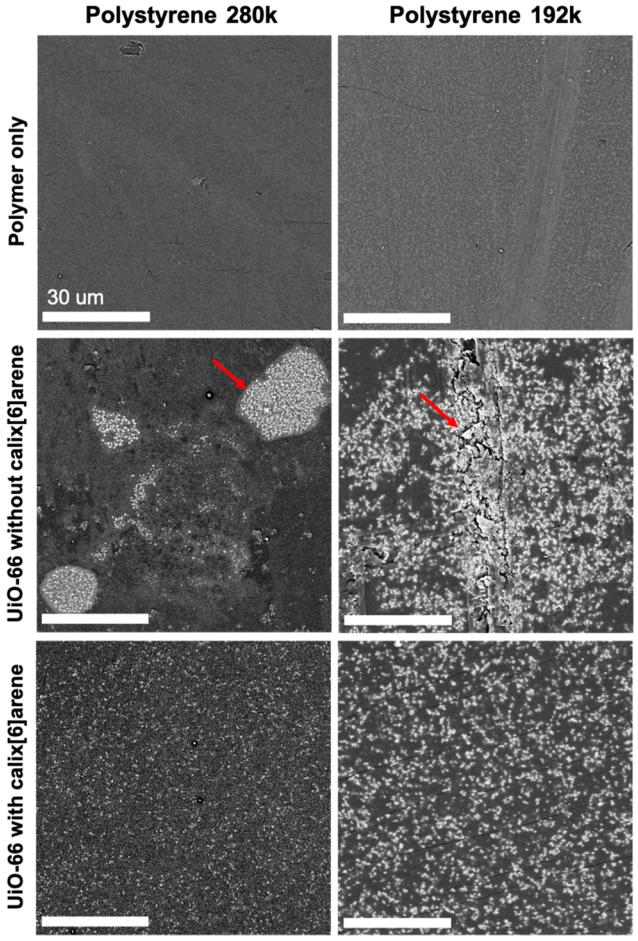

Figure 4. SEM images of UIO-66 and polystyrene (two molecular weights) mixed-matrix films with or without calix[6]arene coating. Scale bars are 30 μm.

■ ASSOCIATED CONTENT

Supporting Information

The Supporting Information is available free of charge on the ACS Publications website at DOI: 10.1021/jacs.9b04198.

Experimental details and additional results of characterizations (PDF)

Time resolved stability of the solutions (MP4)

■ AUTHOR INFORMATION

Corresponding Author

*yavuz@kaist.ac.kr

ORCID

Uiseok Jeong: 0000-0002-2865-5936

J. Fraser Stoddart: 0000-0003-3161-3697

Cafer T. Yavuz: 0000-0003-0580-3331

Notes

The authors declare no competing financial interest.

■ ACKNOWLEDGMENTS

This work was supported by the National Research Foundation of Korea (NRF) under grants funded by the Korean government (MSIP) (No. NRF-2016R1A2B4011027, NRF-2017M3A7B4042140, and NRF-2017M3A7B4042235). We thank Dr. Margaret Schott of Northwestern University for professional editing.

■ REFERENCES

(1) Yavuz, C. T.; Mayo, J. T.; Yu, W. W.; Prakash, A.; Falkner, J. C.; Yean, S.; Cong, L. L.; Shipley, H. J.; Kan, A.; Tomson, M.; Natelson, D.; Colvin, V. L. Low-Field Magnetic Separation of Monodisperse Fe_3O_4 Nanocrystals. *Science* **2006**, *314*, 964−967.

(2) Cook, T. R.; Zheng, Y. R.; Stang, P. J. Metal-Organic Frameworks and Self-Assembled Supramolecular Coordination Complexes: Comparing and Contrasting the Design, Synthesis, and Functionality of Metal-Organic Materials. *Chem. Rev.* **2013**, *113*, 734−777.

(3) Zhou, H. C.; Long, J. R.; Yaghi, O. M. Introduction to Metal-Organic Frameworks. *Chem. Rev.* **2012**, *112*, 673−674.

(4) Farha, O. K.; Eryazici, I.; Jeong, N. C.; Hauser, B. G.; Wilmer, C. E.; Sarjeant, A. A.; Snurr, R. Q.; Nguyen, S. T.; Yazaydin, A. O.; Hupp, J. T. Metal-Organic Framework Materials With Ultrahigh Surface Areas: Is the Sky the Limit? *J. Am. Chem. Soc.* **2012**, *134*, 15016−15021.

(5) Martin, R. L.; Haranczyk, M. Exploring Frontiers of High Surface Area Metal−Organic Frameworks. *Chem. Sci.* **2013**, *4*, 1781−1785.

(6) Furukawa, H.; Ko, N.; Go, Y. B.; Aratani, N.; Choi, S. B.; Choi, E.; Yazaydin, A. O.; Snurr, R. Q.; O'Keeffe, M.; Kim, J.; Yaghi, O. M. Ultrahigh Porosity in Metal-Organic Frameworks. *Science* **2010**, *329*, 424−428.

(7) Thallapally, P. K.; Tian, J.; Radha Kishan, M.; Fernandez, C. A.; Dalgarno, S. J.; McGrail, P. B.; Warren, J. E.; Atwood, J. L. Flexible (Breathing) Interpenetrated Metal−Organic Frameworks for CO_2 Separation Applications. *J. Am. Chem. Soc.* **2008**, *130*, 16842−16843.

(8) Zheng, J.; Vemuri, R. S.; Estevez, L.; Koech, P. K.; Varga, T.; Camaioni, D. M.; Blake, T. A.; McGrail, B. P.; Motkuri, R. K. Pore-Engineered Metal-Organic Frameworks with Excellent Adsorption of Water and Fluorocarbon Refrigerant for Cooling Applications. *J. Am. Chem. Soc.* **2017**, *139*, 10601−10604.

(9) Tsuruoka, T.; Mantani, K.; Miyanaga, A.; Matsuyama, T.; Ohhashi, T.; Takashima, Y.; Akamatsu, K. Morphology Control of Metal-Organic Frameworks Based on Paddle-Wheel Units on Ion-Doped Polymer Substrate Using an Interfacial Growth Approach. *Langmuir* **2016**, *32*, 6068−73.

(10) Chi, W. S.; Roh, D. K.; Lee, C. S.; Kim, J. H. A Shape- and Morphology-Controlled Metal Organic Framework Template for High-Efficiency Solid-State Dye-Sensitized Solar Cells. *J. Mater. Chem. A* **2015**, *3*, 21599−21608.

(11) Lee, H. J.; We, J.; Kim, J. O.; Kim, D.; Cha, W.; Lee, E.; Sohn, J.; Oh, M. Morphological and Structural Evolutions of Metal-Organic Framework Particles from Amorphous Spheres to Crystalline Hexagonal Rods. *Angew. Chem., Int. Ed.* **2015**, *54*, 10564−10568.

(12) Wang, H. L.; Yeh, H.; Chen, Y. C.; Lai, Y. C.; Lin, C. Y.; Lu, K. Y.; Ho, R. M.; Li, B. H.; Lin, C. H.; Tsai, D. H. Thermal Stability of Metal-Organic Frameworks and Encapsulation of CuO Nanocrystals for Highly Active Catalysis. *ACS Appl. Mater. Interfaces* **2018**, *10*, 9332−9341.

(13) Kang, I. J.; Khan, N. A.; Haque, E.; Jhung, S. H. Chemical and Thermal Stability of Isotypic Metal-Organic Frameworks: Effect of Metal Ions. *Chem. - Eur. J.* **2011**, *17*, 6437−6442.

(14) Li, Y.; Ju, Z.; Wu, B.; Yuan, D. A Water and Thermally Stable Metal−Organic Framework Featuring Selective CO_2 Adsorption. *Cryst. Growth Des.* **2013**, *13*, 4125−4130.

(15) Huang, Y. B.; Liang, J.; Wang, X. S.; Cao, R. Multifunctional Metal-Organic Framework Catalysts: Synergistic Catalysis and Tandem Reactions. *Chem. Soc. Rev.* **2017**, *46*, 126−157.

(16) Duan, J.; Chen, S.; Zhao, C. Ultrathin Metal-Organic Framework Array for Efficient Electrocatalytic Water Splitting. *Nat. Commun.* **2017**, *8*, 15341.

(17) Patel, P.; Parmar, B.; Kureshy, R. I.; Khan, N. H.; Suresh, E. Amine-Functionalized Zn(II) MOF as an Efficient Multifunctional Catalyst for CO_2 Utilization and Sulfoxidation Reaction. *Dalton Trans.* **2018**, *47*, 8041−8051.

(18) Jagadeesh, R. V.; Murugesan, K.; Alshammari, A. S.; Neumann, H.; Pohl, M. M.; Radnik, J.; Beller, M. MOF-Derived Cobalt

DOI: 10.1021/jacs.9b04198
J. Am. Chem. Soc. 2019, 141, 12182−12186

Nanoparticles Catalyze a General Synthesis of Amines. *Science* **2017**, *358*, 326−332.
(19) Wu, M. X.; Yang, Y. W. Metal-Organic Framework (MOF)-Based Drug/Cargo Delivery and Cancer Therapy. *Adv. Mater.* **2017**, *29*, 1606134.
(20) Chen, X.; Tong, R.; Shi, Z.; Yang, B.; Liu, H.; Ding, S.; Wang, X.; Lei, Q.; Wu, J.; Fang, W. MOF Nanoparticles with Encapsulated Autophagy Inhibitor in Controlled Drug Delivery System for Antitumor. *ACS Appl. Mater. Interfaces* **2018**, *10*, 2328−2337.
(21) Weston, M. H.; Delaquil, A. A.; Sarjeant, A. A.; Farha, O. K.; Hupp, J. T.; Nguyen, S. T. Tuning the Hydrophobicity of Zinc Dipyridyl Paddlewheel Metal−Organic Frameworks for Selective Sorption. *Cryst. Growth Des.* **2013**, *13*, 2938−2942.
(22) Morris, W.; Wang, S.; Cho, D.; Auyeung, E.; Li, P.; Farha, O. K.; Mirkin, C. A. Role of Modulators in Controlling the Colloidal Stability and Polydispersity of the UiO-66 Metal-Organic Framework. *ACS Appl. Mater. Interfaces* **2017**, *9*, 33413−33418.
(23) Sindoro, M.; Yanai, N.; Jee, A. Y.; Granick, S. Colloidal-Sized Metal-Organic Frameworks: Synthesis and Applications. *Acc. Chem. Res.* **2014**, *47*, 459−469.
(24) Zhang, W.; Hu, Y.; Ge, J.; Jiang, H. L.; Yu, S. H. A Facile and General Coating Approach to Moisture/Water-Resistant Metal-Organic Frameworks with Intact Porosity. *J. Am. Chem. Soc.* **2014**, *136*, 16978−16981.
(25) Yang, S. J.; Park, C. R. Preparation of Highly Moisture-Resistant Black-Colored Metal Organic Frameworks. *Adv. Mater.* **2012**, *24*, 4010−4013.
(26) Li, Z.; Zeng, H. C. Armored MOFs: Enforcing Soft Microporous MOF Nanocrystals with Hard Mesoporous Silica. *J. Am. Chem. Soc.* **2014**, *136*, 5631−5639.
(27) Song, Y.; Thirion, D.; Subramanian, S.; Lah, M. S.; Yavuz, C. T. Monitoring Instability of Linear Amine Impregnated UiO-66 by in-situ Temperature Resolved Powder X-Ray Diffraction. *Microporous Mesoporous Mater.* **2017**, *243*, 85−90.
(28) Jung, J. Y.; Karadas, F.; Zulfiqar, S.; Deniz, E.; Aparicio, S.; Atilhan, M.; Yavuz, C. T.; Han, S. M. Limitations and High Pressure Behavior of MOF-5 for CO_2 Capture. *Phys. Chem. Chem. Phys.* **2013**, *15*, 14319−14327.
(29) Smaldone, R. A.; Forgan, R. S.; Furukawa, H.; Gassensmith, J. J.; Slawin, A. M.; Yaghi, O. M.; Stoddart, J. F. Metal-Organic Frameworks From Edible Natural Products. *Angew. Chem., Int. Ed.* **2010**, *49*, 8630−8634.
(30) Hartlieb, K. J.; Peters, A. W.; Wang, T. C.; Deria, P.; Farha, O. K.; Hupp, J. T.; Stoddart, J. F. Functionalised Cyclodextrin-Based Metal-Organic Frameworks. *Chem. Commun.* **2017**, *53*, 7561−7564.
(31) Bew, S. P.; Burrows, A. D.; Duren, T.; Mahon, M. F.; Moghadam, P. Z.; Sebestyen, V. M.; Thurston, S. Calix[4]arene-Based Metal-Organic Frameworks: Towards Hierarchically Porous Materials. *Chem. Commun.* **2012**, *48*, 4824−4826.
(32) Li, Q. W.; Zhang, W. Y.; Miljanic, O. S.; Sue, C. H.; Zhao, Y. L.; Liu, L. H.; Knobler, C. B.; Stoddart, J. F.; Yaghi, O. M. Docking in Metal-Organic Frameworks. *Science* **2009**, *325*, 855−859.
(33) Zhang, H.; Zou, R.; Zhao, Y. Macrocycle-Based Metal-Organic Frameworks. *Coord. Chem. Rev.* **2015**, *292*, 74−90.
(34) Moradi, M.; Tulli, L. G.; Nowakowski, J.; Baljozovic, M.; Jung, T. A.; Shahgaldian, P. Two-Dimensional Calix[4]arene-based Metal-Organic Coordination Networks of Tunable Crystallinity. *Angew. Chem., Int. Ed.* **2017**, *56*, 14395−14399.
(35) Schulz, M.; Gehl, A.; Schlenkrich, J.; Schulze, H. A.; Zimmermann, S.; Schaate, A. A Novel Calixarene-Based MOF for Highly Selective NO_2 Detection. *Angew. Chem., Int. Ed.* **2018**, *57*, 12961−12965.
(36) Katz, M. J.; Brown, Z. J.; Colon, Y. J.; Siu, P. W.; Scheidt, K. A.; Snurr, R. Q.; Hupp, J. T.; Farha, O. K. A Facile Synthesis of UiO-66, UiO-67 and Their Derivatives. *Chem. Commun.* **2013**, *49*, 9449−9451.
(37) Bárcia, P. S.; Guimarães, D.; Mendes, P. A. P.; Silva, J. A. C.; Guillerm, V.; Chevreau, H.; Serre, C.; Rodrigues, A. E. Reverse Shape Selectivity in the Adsorption of Hexane and Xylene Isomers in MOF UiO-66. *Microporous Mesoporous Mater.* **2011**, *139*, 67−73.
(38) Harrowfield, J. M.; Ogden, M. I.; Skelton, B. W.; White, A. H. Cluster Control in Oligouranyl Complexes of *p-t*-butylcalix[8]arene. *Dalton Trans.* **2010**, *39*, 8313−8318.
(39) Mendoza-Espinosa, D.; Rheingold, A. L.; Hanna, T. A. Synthesis of Bismuth and Antimony Complexes of the "Larger" Calix[n]arenes (n = 6−8); From Mononuclear to Tetranuclear Complexes. *Dalton Trans.* **2009**, 5226−5238.
(40) Gibson, V. C.; Redshaw, C.; Elsegood, M. R. J. Novel Tungsten Calix[8]arene Complexes. *Chem. Commun.* **2002**, 1200−1201.
(41) Silvera Batista, C. A.; Larson, R. G.; Kotov, N. A. Nonadditivity of Nanoparticle Interactions. *Science* **2015**, *350*, 1242477.
(42) Sabetghadam, A.; Seoane, B.; Keskin, D.; Duim, N.; Rodenas, T.; Shahid, S.; Sorribas, S.; Le Guillouzer, C.; Clet, G.; Tellez, C.; Daturi, M.; Coronas, J.; Kapteijn, F.; Gascon, J. Metal Organic Framework Crystals in Mixed-Matrix Membranes: Impact of the Filler Morphology on the Gas Separation Performance. *Adv. Funct. Mater.* **2016**, *26*, 3154−3163.

DOI: 10.1021/jacs.9b04198
J. Am. Chem. Soc. 2019, 141, 12182−12186